



UNITED NATIONS
UNIVERSITY

UNU-GTP

Geothermal Training Programme

Orkustofnun, Grensasvegur 9,
IS-108 Reykjavik, Iceland

Reports 2015
Number 29

TEMPERATURE AND PRESSURE ANALYSIS OF WELLS NJ-13 AND NJ-28 IN THE NESJAVELLIR GEOTHERMAL SYSTEM, SW-ICELAND

Aloysius Tunu Otmar

Mineral Resources Authority

Mining Haus, Poreporena Freeway, P O Box 1906,

Port Moresby 121, National Capital District

PAPUA NEW GUINEA

aotmar@mra.gov.pg

ABSTRACT

Temperature and pressure analysis of geothermal wells is one of the vital steps in evaluating a geothermal reservoir during exploration, production and monitoring the wells. By analysing temperature and pressure logs from the warm up period of a well, the formation temperature and initial pressure can be deduced. Injection well testing is usually done at the end of drilling to find out physical parameters of the well and the reservoir surrounding it and get information on the connection of the well to the reservoir.

Well NJ-13 is a 1609 m deep vertical production well drilled in 1985. It is located in the Nesjavellir high-temperature geothermal field of the Hengill geothermal system located in SW-Iceland. The total enthalpy of well NJ-13 is around 2500 kJ/kg. At well head pressure (P_0) of 16 bar-g, the power output for well NJ-13 is 15 MWe, as estimated from the original production test data.

Well NJ-28 is a directional well drilled from the same well pad as NJ-13 in May-June 2015 as a makeup well to a depth of 1301 m with respect to the platform. The intended depth of this well was 2100 m but the drilling was stopped at 1301 m after several attempts to continue when the drill string repeatedly got stuck due to intrusions at the bottom of the well. The total enthalpy of well NJ-28 is around 2600 kJ/kg. At a well head pressure (P_0) of 20 bar-g, the power output of well NJ-28 is 5 MWe estimated from production test data from September 2015. Well NJ-28 has lower transmissivity and injectivity than well NJ-13 which might explain why NJ-28 is a poor producer compared to NJ-13.

1. INTRODUCTION

This paper is written as a final project report of the six-month training at the United Nations University Geothermal Training Programme in 2015. The report presents analysis of temperature and pressure logs from wells NJ-13 and NJ-28 from the Nesjavellir geothermal field. The available pressure and temperature logs from their warm up periods were used to deduce the formation temperature and initial

pressure in the wells. Additionally, injection and production well tests were analysed to find relevant parameters of the geothermal reservoir around the wells.

The Nesjavellir geothermal field is situated at the northern margin of the Hengill geothermal system in SW-Iceland (Figure 1A). There are several other high-temperature geothermal fields within Hengill geothermal system, such as Hellisheidi and Hverahlíð which lie further towards the south (Figure 1B), Gráuhnjúkar towards the southwest and Bitra towards the south east. The data analysed and presented in this report is from Orka Náttúrunnar (ON Power), which operates the Nesjavellir geothermal field. The Nesjavellir geothermal power plant's output is 120 MWe and 300 MWt (2014).

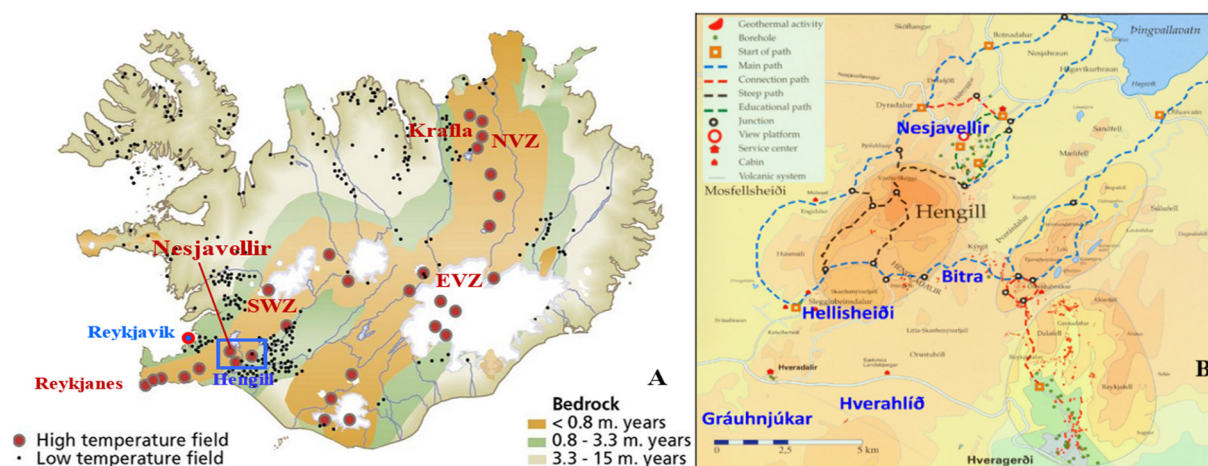


FIGURE 1: A) Geological map of Iceland, with geological zones, low- and high-temperature geothermal fields, and main volcanic zones (modified after Jóhannesson and Saemundsson, 1999), NVZ – Northern Volcanic Zone, EVZ – Eastern Volcanic Zone, SWZ – Southwestern Volcanic Zone; B) Hengill volcanic system, SW-Iceland and its geothermal fields (Gislason and Gunnlaugsson, 2003)

2. BACKGROUND

2.1 Regional geology

With about thirty active volcanic systems and numerous geothermal systems, the island of Iceland is located on the northern part of the diverging Mid-Atlantic Ridge between the North American and Eurasian plate (Saemundsson, 1979). The two plates are moving away from each other at a rate of 15 mm/year (Árnadóttir et al. 2008). The active spreading of the ridge and the Icelandic mantle plume enhance magma flow from the earth's interior to the surface or as intrusions at shallow levels, which react with groundwater resulting in the formation of the highly prospective geothermal systems in Iceland.

Iceland can be divided into three (3) main geological zones depending on the age of the basaltic rocks. These three main active volcanic zones of Iceland, as identified by Nielsson and Franzson (2010), are: the south-western volcanic zone (SWZ), which includes the Hengill and Reykjanes volcanic systems, the eastern volcanic zone (EVZ) and the northern volcanic zone (NVZ) as shown in Figure 1A.

Most of the high-temperature geothermal fields of Iceland are located inside the volcanic zones, which are covered with late Quaternary basalts (less than 0.8 million years old) and hyaloclastites trending NE-SW. Low-temperature geothermal fields are mainly scattered on the peripheries of these areas and further away, indicated by the black dots in Figure 1A.

2.2 Geology of Hengill geothermal area

The Nesjavellir high-temperature geothermal field is ~30 km ESE of Reykjavík on the northern margin of the Hengill area, which hosts one of the largest high-temperature geothermal systems in Iceland, extending over 50 km² and located in the south western volcanic zone (Figure 1A). The tensional stress that has developed as a result of the structural activity in the area has opened up NE-SW trending vertical fractures creating permeable zones for the outflow of thermal fluids (Franzson and Sigvaldason, H., 1985). These thermal fluids are heated through shallow crustal magma at temperatures of approx. 1200°C (Bödvarsson et al., 1990).

The Hengill area is comprised entirely of late Quaternary and Postglacial volcanic rocks mostly of basaltic flows and hyaloclastites and minor deposits of rhyolites. Árnason et al. (1967) stated that the Nesjavellir field features a 10 km broad graben trending NE-SW.

2.3 Surface geophysical exploration of Hengill area

Surface geophysical exploration studies of the Hengill area have been undertaken since 1964, including Nesjavellir and other geothermal fields in the Hengill area. The most advanced and informative exploration methods used to image the Hengill geothermal system as well as other geothermal areas in Iceland prior to drilling are resistivity measurements. Recent studies include TEM and MT electromagnetic soundings, which were integrated through a joint inversion, in order to construct a comprehensive map of resistivity from the surface down to over 15 km depth (Árnason et al., 2010).

Figure 2 shows the resistivity at 850 m below sea level and the density of seismic events in the Hengill geothermal system. A joint inversion of TEM and MT data from 148 sounding stations in the Hengill area reveals a resistivity structure consisting of a shallow low-resistivity layer in the upper most 2 km, underlain by high resistivity.

The resistivity structures are related to variations in hydrothermal alteration which appear to be of greater importance than the temperature variation. The low-temperature clay-rich outer margin of a high-temperature reservoir is characterized by low resistivity while the underlying higher resistivity is associated with the formation of chlorite (formation temperature >230°C) and less water-rich alteration mineral assemblages (Árnason et al. 2010). At greater depth a second low-resistivity layer is observed in most parts of the area, again underlain by higher resistivity. The depth to this second low-resistivity layer varies over the Hengill area. It is seen at its shallowest depth (about 3 km) under and around Mount Hengill. The nature of the second low-resistivity layer is not well known.

Figure 3 shows a cross-section of the alteration zones of Nesjavellir high-temperature geothermal system and the main permeability structures.

2.4 The Nesjavellir geothermal field

Exploration drilling of the Nesjavellir geothermal field started in 1964 and drilling was continued with intervals until 1986, when a total of eighteen wells had been drilled. Construction of the Nesjavellir power plant was started in 1987. The power plant was officially opened on the 29th September 1990 (Gunnarsson et al., 1992).

In October 2015, a total of 28 wells have been drilled. In May-June 2015, a new makeup well, NJ-28, was drilled from the same well pad as production well NJ-13. Thirteen of these wells are commercial producers with an output of 120 MWe and 300 MWth (2014). The rest of the wells are either used for re-injection, or are shut-in or abandoned wells (Franzson and Steingrímsson, 2015).

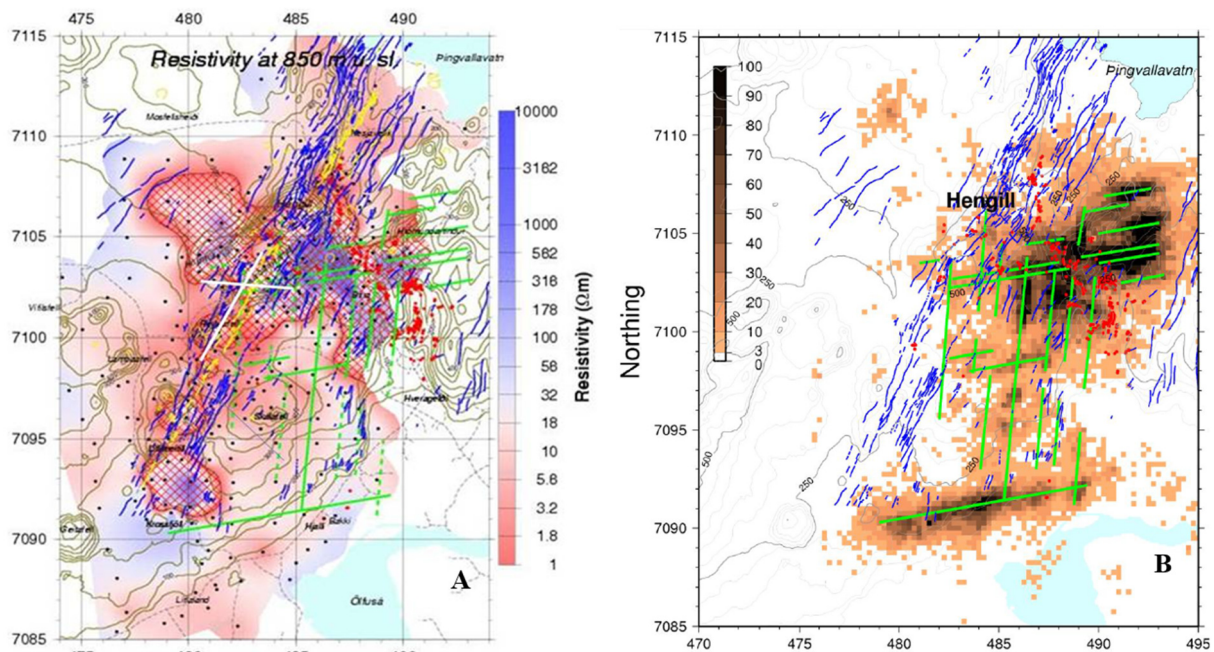


FIGURE 2: A) Resistivity map of Hengill and surroundings at 850 m b.s.l. based on inversion of TEM and MT data; low resistivity ($<10\Omega$) is red and high is blue, while the cross-hatched areas define high resistivity bodies below the low resistivity indicating alteration temperatures of over 230°C . Geothermal manifestations are marked by red dots, TEM and MT stations by black dots, mapped and inferred faults or fractures are blue and green respectively and volcanic craters and fissures are marked yellow (from Árnason et al., 2010). B) Seismicity of the Hengill central volcano from 1991 to 2001; inferred faults and fractures are symbolized by green straight lines (Árnason et al., 2010, modified from Árnason, and Magnússon, 2001)

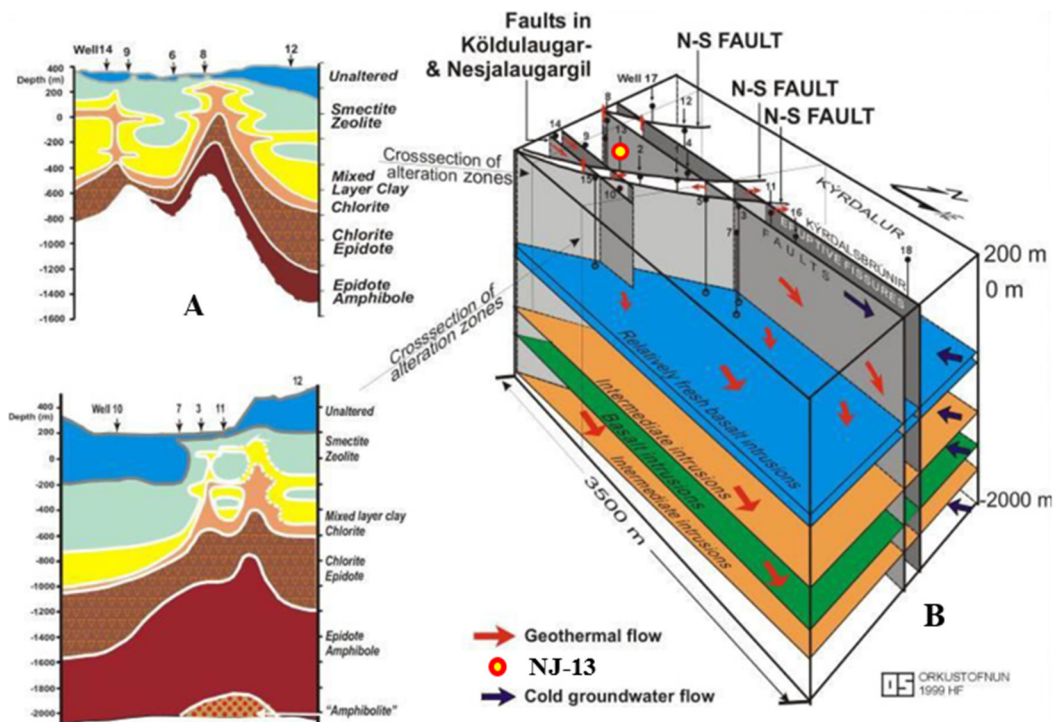


FIGURE 3: A) Cross-section of alteration zones in the Nesjavellir high-temperature system; B) Main permeability structure (Franzson and Steingrímsson, 2015)

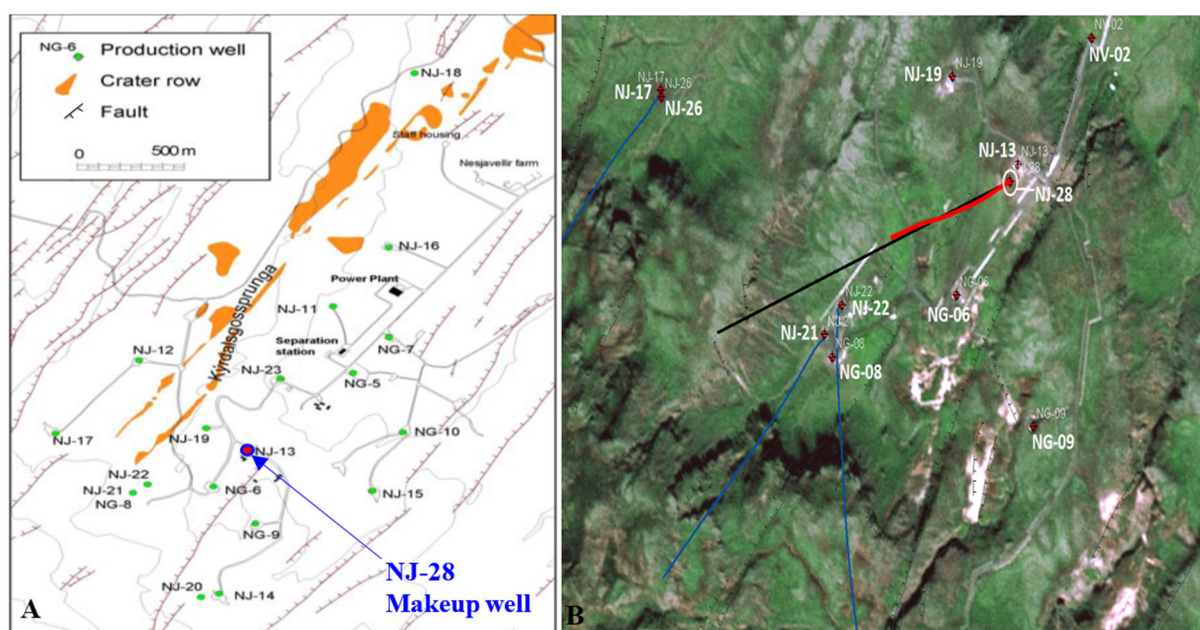


FIGURE 4: A) Nesjavellir geothermal field (Gíslason, 2000); B) Trajectory of well NJ-28 projected on the surface is indicated by a red line (Gunnarsdóttir et al., 2015)

A map of the Nesjavellir geothermal field with the locations of wells NJ-13 and NJ-28 is shown in Figure 4. It also shows the trajectory of well NJ-28 towards the west-southwest (Gunnarsdóttir et al., 2015).

3. ANALYSIS OF FORMATION TEMPERATURE AND INITIAL PRESSURE

Formation temperature and initial pressure are important information for each well and they are deduced from well logs during warm up. During drilling, injection of cold water cools the surrounding formations and then the well is left for a few months to recover to the initial temperature and pressure condition of the surroundings. This recovery period is known as the ‘warm-up’ period. Measurements of temperature and pressure are done during drilling, warm-up period and as a part of regular reservoir monitoring. Temperature logs during drilling and warm-up are analysed to provide information on the location of feed zones, relationship between these zones and the relative size (permeability) of the individual feed zones.

Different methods are used to estimate the formation temperature and initial pressure of the formation. For the formation temperature estimation, two methods are commonly used as an aid in determining the formation temperature, i.e. the Horner plot and the Albright methods.

The Horner plot method, which is incorporated in the BERGHITI of the ICEBOX (Arason et al., 2004) software, was used in this project and is described below. After defining the formation temperature, the corresponding initial pressure was estimated using the PREDYP programme of the ICEBOX software.

3.1 The Horner plot method

The Horner plot uses an empirical equation to estimate the formation temperature for relatively long recovery periods, usually ranging from weeks to months (Dowdle and Cobb, 1975). This method

assumes a straight line between the maximum wellbore temperature and the natural logarithm of the relative time, τ or *Horner time*, as described in Equation 1 below:

$$\tau = \left(\frac{t_0 + \Delta t}{\Delta t} \right) \text{ Horner time} \quad (1)$$

where Δt = Time passed since last circulation stopped;
 t_0 = Circulating time.

Equation 1 is incorporated into the BERGHITI software and is used to find the formation temperature at a selected depth as a function of $\ln(\tau)$ and then plot a straight line through the temperature measurements (t,T) in which the formation temperature is estimated by extrapolation to $\tau = 1$ (Helgason, 1993). Figure 1 in Appendix I shows an example of how the formation temperature is determined using the BERGHITI software. The dots are temperature readings taken at different dates and the green line joins the two later temperature values where the formation temperature is determined from the y-axis at the top right hand corner.

3.2 Initial pressure - introduction

Initial pressure is the reservoir pressure estimated from data obtained during the recovery period of the well. The warm-up pressure profiles are plotted to determine their intersection known as the ‘pivot point’ which is the initial or reservoir pressure for the dominating feed zone. For two or more dominating feed zones, the pivot point represents the average pressure condition between these feed zones. If the formation temperature and pivot point pressure is known, the PREDYP program from ICEBOX (Arason et al., 2004) which computes pressure in a static water column, can be used to calculate the initial pressure in the well, depending on the corresponding formation temperature, by adjusting the depth-pressure-curve to the known pressure at the pivot point.

3.3 Temperature and pressure profiles

The temperature and pressure conditions of wells NJ-13 and NJ-28 are analysed and interpreted with the purpose of understanding their formation temperature and initial pressure. Temperature and pressure measurements for NJ-13 and NJ-28 taken during warm up and end of drilling and presented by Steingrímsson et al., (1986), and Gunnarsdóttir et al., (2015), respectively, are analysed in this report. The temperature and pressure profiles for both wells are presented in this section. Table 1 shows the borehole dimensions of both NJ-13 and NJ-28.

TABLE 1: Borehole dimensions for wells NJ-13 and NJ-28

Borehole No	Year drilled	Total depth w.r.t. platform (m)	Section	Casing diameter (in)	Casing depth w.r.t. platform (m)	ISN 93 coordinates (X, Y, Z)
NJ-13	1985	1609	Surface	18 5/8	63	389319, 401490, 287
			1	13 3/8	277.55	
			2	9 5/8	816.85	
			3	7	1595.9	
NJ-28	2015	1301	Surface	18 5/8	98.3	389319, 401490, 287
			1	13 3/8	316.9	
			2	9 5/8	801.2	
			3	7	1290.6	

3.3.1 Well NJ-13

Well NJ-13 is a vertical well, drilled in 1985, to a measured depth of 1609 m with respect to the drilling platform. Hyaloclastites and lava flows were dominant down to 500 m. Intrusions are rather common below 700 m depth where most of the feed points are located similar to other wells at Nesjavellir (Steingrímsson et al., 1986). Loss of circulation was observed in feed points high up in the well, but little or no loss at 300-800 m depth where the system seems to be over-pressurized. The top pressure in the production zone from 800 m down was on the other hand under-pressurized. When the well was closed the pressure was around or above 85 bar, so the well was left open, constantly blowing for a period of time. It was also shut in for a short while when well NJ-28 was connected to the pipe system.

Figure 5 shows temperature and pressure logs as well as the formation temperature and initial pressure. According to Steingrímsson et al. (1986), several feed points were identified in NJ-13 from the temperature logs measured during and after drilling. The feed points identified from these T-logs are at 940, 1070, 1120, 1150, 1190, 1363, 1500 and 1540 m depth. The largest feed point detected was at 940 m but the one at 1120 m also showed rapid warm-up. The main feed point where total loss of circulation was noticed during drilling is at 1363 m depth. This does not appear on the temperature log but it is worth mentioning that the well was cooled down to 1300 m depth while logging the temperature before finishing the drilling.

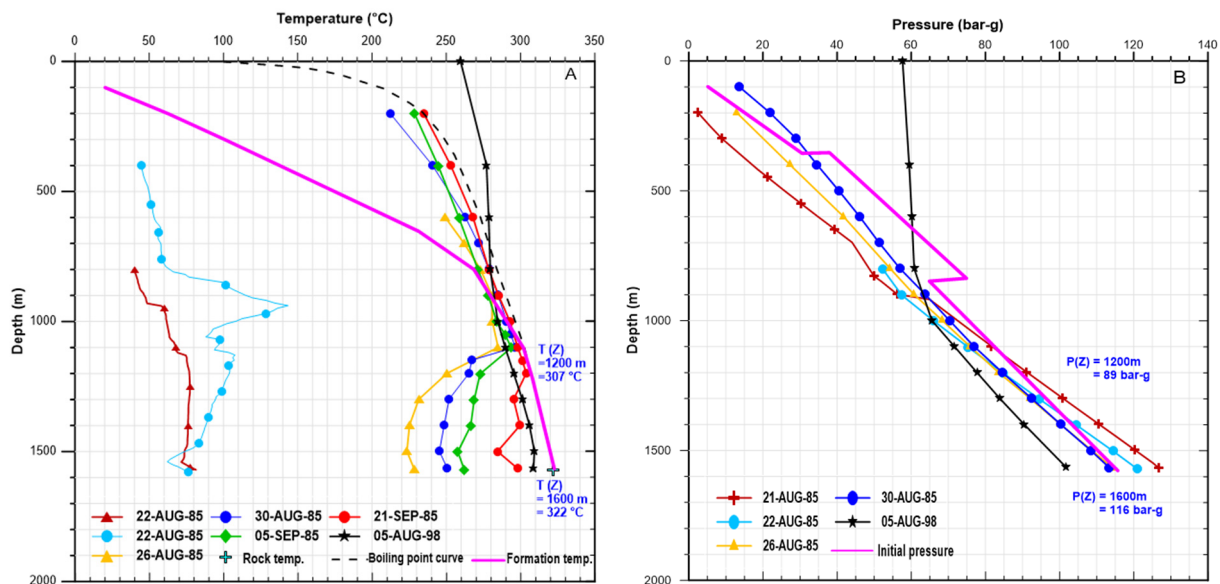


FIGURE 5: A) Temperature logs, boiling point curve and formation temperature; and
B) Pressure logs, boiling point pressure and initial pressure from well NJ-13

The inversed temperature profiles from 1100-1500 m indicate cooling due to water circulation during drilling. The BERGHITI software was used to determine the formation temperature by inserting the temperature values at selected depths from the four warm-up measurements on 26th August to 21st September 1985 and reading from the Horner plots. The measurements from 5th August 1998 were not used for this analysis but for comparison. The formation temperatures estimated using BERGHITI are 307°C at 1200 m and 322°C at 1600 m depth.

3.3.2 Well NJ-28

Well NJ-28 is a directional well drilled from the same well pad as NJ-13 in May-June 2015 to a measured depth of 1301 m with respect to the drill platform which corresponds to 1160 m vertical depth from the surface. Hyaloclastites are dominant down to 1044 m followed by lava flows down to 1280 m, underlain by another lava flow formation to the bottom of the well.

The intended depth of this well was 2100 m but the drilling was stopped after several attempts to continue when the drill string reportedly got stuck. This is believed to be due to an intrusion at the bottom of the well. Circulation loss was first detected at 1086 m depth and at the end of drilling it was 25 l/s, but increased up to 80 l/s during the process of trying to release the drill string.

Figure 6 shows the temperature and pressure logs for NJ-28. Only two (2) temperature and pressure logs were measured during warm-up on the 10th July and 04th August 2015. These two measurements were used to determine the formation temperature and initial pressure of well NJ-28. The main feed zone of well NJ-28 is located at the bottom of the well. Though it wasn't possible to precisely locate the largest feed point(s), several smaller feed points were observed at 820, 900, 1020 and 1060 m depth (Gunnarsdóttir et al., 2015).

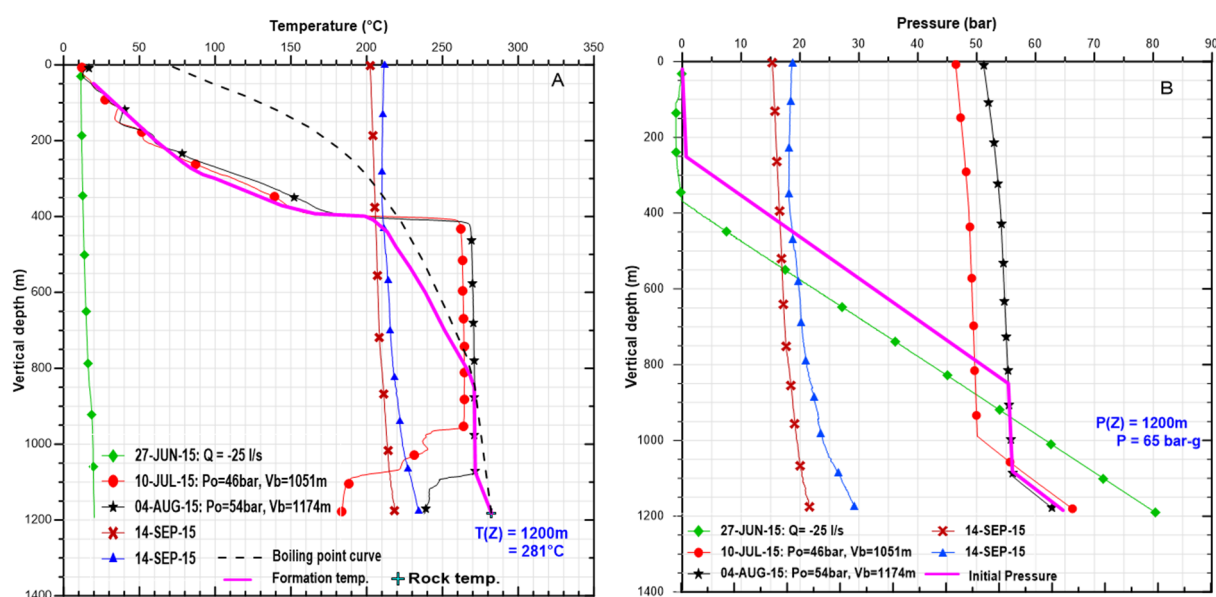


FIGURE 6: A) Temperature logs, boiling point curve and formation temperature;
B) Pressure logs, boiling point pressure and initial pressure from well NJ-28

The inversed temperature profiles from 950 m indicate cooling due to circulation during drilling. The temperature logs for NJ-28 are most likely affected by other nearby production wells including NJ-13 and NG-6 which is located 300 m southwest of NJ-13. Since there were only two measurements done during warm-up, the formation temperature could not be determined using BERGHITI. It was deduced by assuming that the initial pressure value at 1200 m depth was between those given by the two pressure profiles measured on the 10th July and the 04th August 2015. The initial pressure is estimated to be 65 bar-g with corresponding boiling point temperature of 281°C estimated from the steam table. These values are 24 bar-g and 26°C less than that of NJ-13 at the same depth of 1200 m.

The great pressure difference between the estimated initial pressures of the wells is due to utilization of geothermal energy from NJ-13 and the other wells nearby. The difference is both caused by drawdown in the reservoir (production response) and by the fact that nearby wells (NJ-13 and NG-6) are in production at the same time as the well is measured. It is recommended to do some additional measurements during its warm-up period to fully understand the characteristics of well NJ-28.

The well is at boiling conditions from the bottom up to 1075 m, then there is a steam cap up to a depth of 850 m with a pressure of 56 bar-g and a corresponding temperature of 271°C. The corresponding boiling point temperatures from the steam tables for each initial pressure value at the respective depths were plotted to determine the formation temperature curve. Figure 6 shows the temperature and pressure logs for NJ-28, including the estimated formation temperature and initial pressure. The temperature and pressure profiles measured on the 14th September 2015 during production obviously indicate boiling down the well (Figure 6).

4. WELL INJECTION TEST

4.1 Theoretical overview of injection well testing

The main aim of injection well tests is to investigate the physical parameters of the well and the reservoir that control the response of the reservoir with respect to pressure changes caused by the injection. During injection well testing, fresh water is injected gradually into the well to change the water level until a steady height is reached. The pressure response is recorded as a function of time.

The pressure diffusion equation forms the basis of all models in well testing theory that are used to calculate the pressure response in the reservoir at a certain distance (r) from the well after a given time (t) with constant injection (or production). The three main laws that are used in deriving the pressure diffusion equation are conservation of mass, conservation of momentum (Darcy's Law) and fluid compressibility equation which describes the state of the reservoir fluid. Each of these laws is described below.

i) *Law of conservation of mass:*

Mass in – Mass out = Rate of change of mass, or

$$\left(\rho Q + \frac{\partial(\rho Q)}{\partial r} dr \right) - \rho Q = 2\pi r dr \frac{\partial(\rho \phi h)}{\partial t} \quad (2)$$

where ρ = Density of fluid (kg/m³);
 Q = Mass flow (kg/s);
 h = Reservoir thickness (m);
 ϕ = Porosity (ratio, $0 < \phi < 1$);
 r = Distance from the centre of the well to the cylindrical shell; and
 dr = Thickness of the shell.

ii) *Law of conservation of momentum (Darcy's Law)*

$$Q = \frac{2\pi r h k}{\mu} \frac{\partial p}{\partial r} \quad (3)$$

where k = Permeability (m²);
 μ = Fluid viscosity (Pa s); and
 $\frac{\partial p}{\partial r}$ = Pressure gradient (Pa/m);.

iii) *Compressibility (relative volume change as a response to pressure)*

$$C_t = \phi C_w + (1 - \phi) C_r \text{ where } C_r = \frac{1}{1 - \phi} \frac{\partial \phi}{\partial p} \text{ and } C_w = \frac{1}{\rho} \frac{\partial \rho}{\partial p} \quad (4)$$

where C_r = Rock compressibility (Pa⁻¹);
 C_w = Water compressibility (Pa⁻¹); and
 C_t = Total compressibility (Pa⁻¹).

Depending on the boundary and initial conditions, different solutions to the pressure diffusion equation can be obtained. Assumptions are established through knowledge gained on the reservoir system including the boundary and the initial conditions. Horne (1995) suggested several assumptions, given below for simplification leading to the diffusion equation:

- Horizontal radial flow;
- Application of Darcy's law;
- Homogeneous and isotropic reservoir;
- Isothermal conditions;
- Uniform thickness of reservoir, h ;

- Single-phase flow;
- Small pressure gradients;
- Small and constant compressibility, c_t ;
- Constant porosity, ϕ ;
- Constant fluid viscosity, μ ; and
- Constant permeability, k .

Furthermore, some assumptions are made to get the Theis solution:

- *Initial conditions*

Pressure throughout the reservoir is equal to the initial pressure P_0 :

$$P(r,t) = P_0 \quad \text{for } t = 0, \text{ all } r > 0 \quad (5)$$

- *Boundary conditions*

- Outer boundary

Pressure is equal to the initial pressure at infinity:

$$P(r,t) = P_0 \quad \text{for } r \rightarrow \infty, t > 0 \quad (6)$$

- Inner boundary

Well flow at a constant rate Q (m^3/s):

$$Q = \frac{2\pi kh}{\mu} \lim_{r \rightarrow 0} \left(r \frac{\partial p}{\partial r} \right) \quad \text{for } r \rightarrow 0, t > 0 \quad (7)$$

Given the above assumptions, the three equations for the three laws are combined to give the diffusion equation as follows:

$$\frac{1}{r} \frac{\partial}{\partial r} \left(r \frac{\partial p}{\partial r} \right) = \frac{\mu C_t}{k} \frac{\partial p}{\partial t} = \frac{S}{T} \frac{\partial p}{\partial t} \quad \text{or} \quad \frac{\partial^2 p}{\partial r^2} + \frac{1}{r} \frac{\partial p}{\partial r} = \frac{\mu C_t}{k} \frac{\partial p}{\partial t} = \frac{S}{T} \frac{\partial p}{\partial t} \quad (8)$$

$$\text{using} \quad S = c_t h \quad \text{and} \quad T = \frac{kh}{\mu} \quad (9)$$

where S = Storativity ($\text{m}^3/\text{Pa} \cdot \text{m}^2$); and
 T = Transmissivity ($\text{m}^3/(\text{Pa} \cdot \text{s})$).

The Theis (1935) solution of the radial pressure diffusion equation for these condition (initial and boundary in Equations 5-7) given above is then given by:

$$\Delta P = P(r,t) - P_0 = \frac{Q}{4\pi T} W\left(\frac{Sr^2}{4Tt}\right) = \frac{Q\mu}{4\pi kh} W\left(\frac{-\mu C_t r^2}{4kt}\right) \quad (10)$$

where $W(u)$ is known as the “well function”; and $u = \frac{Sr^2}{4Tt}$, or:

$$W(u) = E_i(-u) = - \int_u^\infty \frac{e^{-x}}{x} dx \quad (11)$$

If $u < 0.01$, Equation 11 can be approximated by: $W(u) \approx -\ln(u) - \gamma \approx -\ln(u) - 0.5772$, with γ known as the Euler constant.

Equation 10 for $t > 25 \frac{Sr^2}{T}$ gives:

$$\Delta P = \frac{2.303Q}{4\pi T} \left[\log\left(\frac{Sr^2}{4Tt}\right) + \frac{\gamma}{2.303} \right] \quad (12)$$

Figure 7 shows the different types of boundaries with their expected responses of the reservoir where pressure is a function of log time. The Theis behaviour describes an infinitely large reservoir with absence of boundary effects. However, the boundary effects will appear in every reservoir (Bödvarsson and Whitherspoon, 1989).

The injection data is analysed and a model is selected including the reservoir boundary properties, reservoir characteristics such as *transmissivity*, *storativity*, *wellbore skin* and *wellbore storage*.

The Well Tester software (Júlíusson et al., 2007) is used to simulate the data using the selected model and iterating to an acceptable solution. Each of these characteristics and parameters are explained mostly word by word in automatic reports made by Well Tester (Júlíusson et al., 2007).

The *storativity* (Equation 9) defines the volume of fluid stored in the reservoir per unit area per unit increase in pressure. It has a great impact on how fast the pressure is transmitted within the reservoir. Because of fluid compressibility, storativity varies significantly between reservoir types; liquid-dominated, two-phase or dry steam. Typical storativity values for liquid-dominated geothermal reservoirs are around $10^{-8} \text{ m}^3 / (\text{Pa} \cdot \text{m}^2)$ while for two-phase reservoirs the values might be in the order of $10^{-5} \text{ m}^3 / (\text{Pa} \cdot \text{m}^2)$.

The *transmissivity* (Equation 9) describes the ability of the reservoir to transmit fluid which affects the pressure gradient between the well and the reservoir. The transmissivity can vary depending on certain geological factors but typical values from injection testing in Icelandic geothermal reservoirs are in the order of $10^{-8} \text{ m}^3 / (\text{Pa} \cdot \text{s})$.

The *injectivity index* (II) is an estimated value which describes the connectivity of the well to the surrounding reservoir. It is given in units of $(\text{l/s})/\text{bar}$ and is defined as the change in injection flow rate divided by the change in stabilized reservoir pressure:

$$II = \frac{\Delta Q}{\Delta P} \quad (13)$$

where II = Injectivity index $(\text{l/s})/\text{bar}$;
 ΔQ = Change of flow rate l/s ; and
 ΔP = Change in pressure bar.

The *skin factor* is a variable describing the permeability of the volume surrounding the well where the permeability is not the same as in the reservoir (Figure 8). The skin zones are often affected by drilling operations such as fracture blockage from the cuttings or mechanically induced fractures. For damaged wells, the *skin factor* is positive and for stimulated wells it is negative.

The skin factor in Icelandic geothermal reservoirs is typically around -1, however values may range from about -5 to 20. When $s < 0$, the well reacts like a wider well or as a stimulated well, if $s > 0$, the well seems narrower and acts like a damaged well (Hjartarson, 1999).

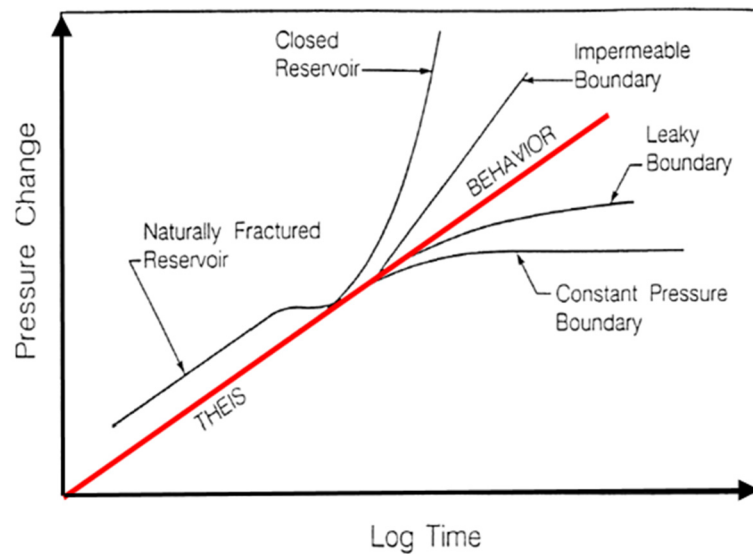


FIGURE 7: Typical pressure responses indicating different reservoir boundaries over log-time (Bödvarsson and Whitherspoon, 1989)

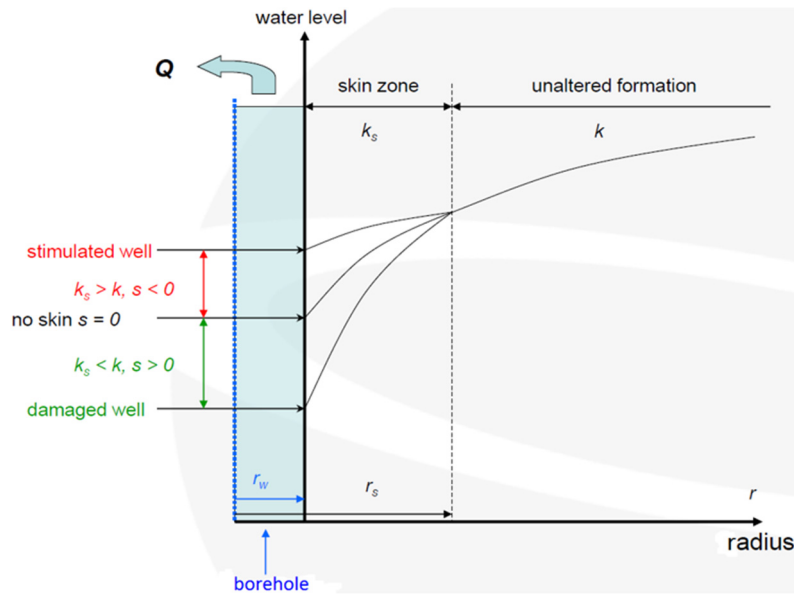


FIGURE 8: Schematic diagram showing pressure changes in the vicinity of a well due to a skin effect where:
 r_w = well radius and r_s = radius of skin
 (modified from Hjartarson, 1999)

The *wellbore storage* C is a property that accounts for the difference between the wellhead flow rate and the “sand face” flow rate (i.e. the flow into or out of the actual formation). Wellbore storage effects can occur in several ways but most commonly by changing the liquid level and fluid expansion. In injection testing the most dominant cause for wellbore storage is a change in liquid level. The storage effect is caused by the volume in the wellbore itself being emptied or filled. Fluid expansion is caused by fluid flow from the well. When the well is first opened to flow, the pressure in the wellbore drops and the fluid in the wellbore expands, providing the initial production volume (Horne, 1995). Typically, under single-

phase liquid conditions the wellbore storage is negligible because of fluid expansion. However, in a geothermal well where the wellbore fluid changes from a single-phase liquid to a two-phase steam-water mixture the expansion effect can be very significant.

4.2 Well injection test analysis and interpretation for NJ-13 and NJ-28

Well injection tests were performed in wells NJ-13 and NJ-28 after the completion of their drilling. All the well test analyses and interpretations were done using Well Tester software (Júlíusson et al., 2007). The software is designed to analyse well test data with respect to the reservoir models selected and the best response is usually selected by comparing the best simulated response, i.e. the generally lowest coefficient of variation C_v , which by Júlíusson et al. (2007): “is defined as the ratio between the standard deviation σ and the mean value μ for the particular parameter in the model:

$$C_v = \frac{\sigma}{\mu}$$

It gives an indication on the spread in the parameter estimate in relation to the estimated parameter value.”

The data manipulation is done by dividing the test into several simple processes that range from setting initial conditions to modelling and giving a final report (Júlíusson et al., 2007). Table 2 shows the well testing model used for all steps for the analysis of both NJ-13 and NJ-28.

TABLE 2: Model selected for both wells NJ-13 and NJ-28

Reservoir	Homogenous
Boundary	Constant pressure
Well	Constant skin
Wellbore	Wellbore storage

4.2.1 Well injection test of NJ-28

An injection test at well NJ-28 was performed on the 27th June 2015. The temperatures and pressures were measured from 20 to 1290 m depth at an initial constant injection rate of 21 l/s after which the sensor was left for a short while to measure the stabilized pressure before starting the first step. Injection at step 1 started with 35 l/s, step 2 with 50 l/s and step 3 with 25 l/s. After the step test, the temperatures and pressures were measured again from the bottom at 1290 m up to 30 m at a constant rate of 25 l/s. Figure 9 shows the pressure responses during each of the three steps.

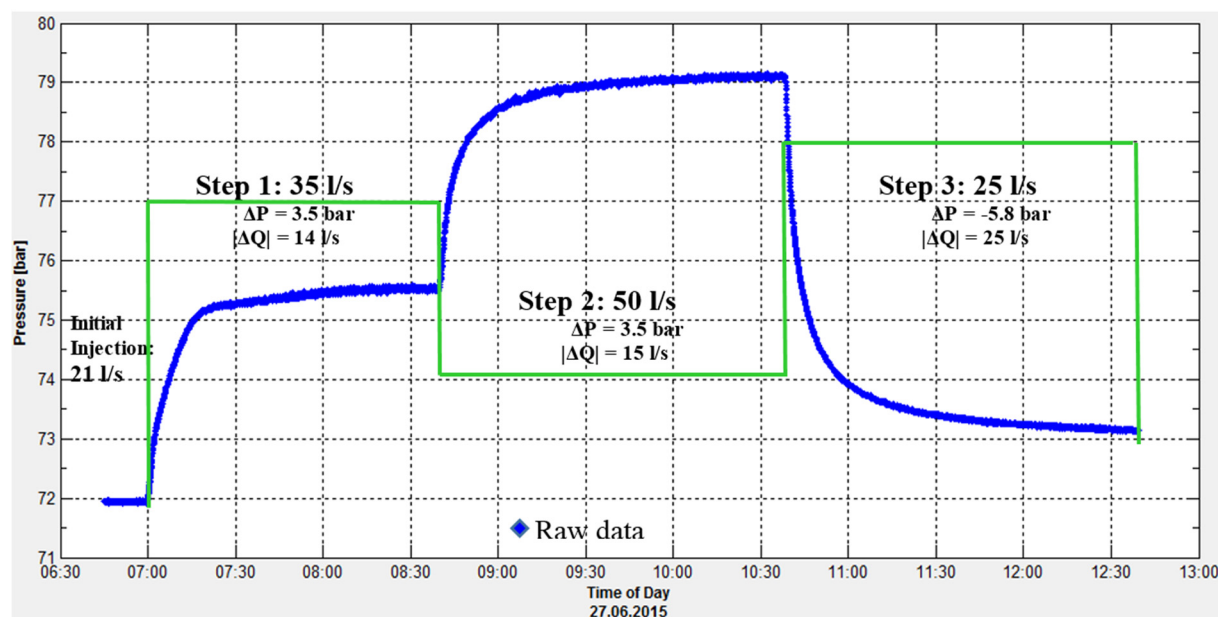


FIGURE 9: Pressure and injection as a function of time in well NJ-28 during injection well test with 3 steps

The initial parameters that were used to calculate the estimated reservoir pressure using Well tester are given in Table 3.

TABLE 3: Summary of initial parameters of well NJ-28

Parameter name	Value	Unit
Estimated reservoir temperature T	280	°C
Estimated reservoir pressure P	75	bar
Wellbore radius r_w	0.12	m
Porosity ϕ	0.1	-
Dynamic viscosity of reservoir fluid μ	9.39×10^{-5}	Pa·s
Compressibility of reservoir fluid c_w	2.17×10^{-9}	Pa ⁻¹
Compressibility of rock matrix c_r	2.44×10^{-11}	Pa ⁻¹
Total compressibility c_t	2.39×10^{-10}	Pa ⁻¹

Each of the steps was separately simulated through a non-linear regression analysis and their respective parameters were estimated using Well Tester software (Table 4).

For comparison, the same data from well NJ-28 was also simulated by selecting a *dual porosity*, *constant pressure boundary*, *constant skin* and *wellbore storage*. Table 5 shows the results simulated by a non-linear regression analysis for a *dual porosity* model.

TABLE 4: Summary of the results from the non-linear regression parameter estimation using injection test data from well NJ-28 for a homogenous model

	Step 1	Step 2	Step 3	Unit
Transmissivity T	3.7×10^{-8}	4.3×10^{-8}	3.5×10^{-8}	$\text{m}^3/(\text{Pa.s})$
Storativity S	2.0×10^{-8}	4.4×10^{-8}	8.6×10^{-8}	$\text{m}^3/(\text{Pa.m}^2)$
Skin factor s	-0.6	-0.4	-0.9	-
Wellbore storage C	1.7×10^{-5}	1.4×10^{-5}	9.8×10^{-6}	m^3/Pa
Injectivity Index II	4.0	4.3	4.3	$(\text{l/s}) / \text{bar}$
Permeability thickness kh	3.4×10^{-12}	4.1×10^{-12}	3.3×10^{-12}	m.m^2

TABLE 5 Summary of results from the non-linear regression parameter estimation using injection test data from well NJ-28 for a dual porosity model

	Step 1	Step 2	Step 3	Unit
Transmissivity T	3.3×10^{-8}	3.7×10^{-8}	3.5×10^{-8}	$\text{m}^3/(\text{Pa.s})$
Storativity S	6.3×10^{-8}	2.4×10^{-8}	8.4×10^{-9}	$\text{m}^3/(\text{Pa.m}^2)$
Skin factor s	-1.1	-1.35	-2.05	-
Wellbore storage C	1.9×10^{-5}	1.5×10^{-5}	1.0×10^{-5}	(m^3/Pa)
Injectivity Index II	3.9	4.3	4.2	$(\text{l/s}) / \text{bar}$
Permeability thickness kh	3.4×10^{-12}	4.1×10^{-12}	3.3×10^{-12}	m.m^2

Step 1 is selected to illustrate the results of the data simulations. They are plotted using Well Tester output figure. The simulated results from Table 4 and 5 were compared and all 3 steps of well NJ-28 turned out to give the best response for the selected model of a *homogenous reservoir, constant pressure boundary, constant skin and wellbore storage*. Figure 10 shows the simulated model, collected data and selected data for step 1 for the homogenous reservoir model.

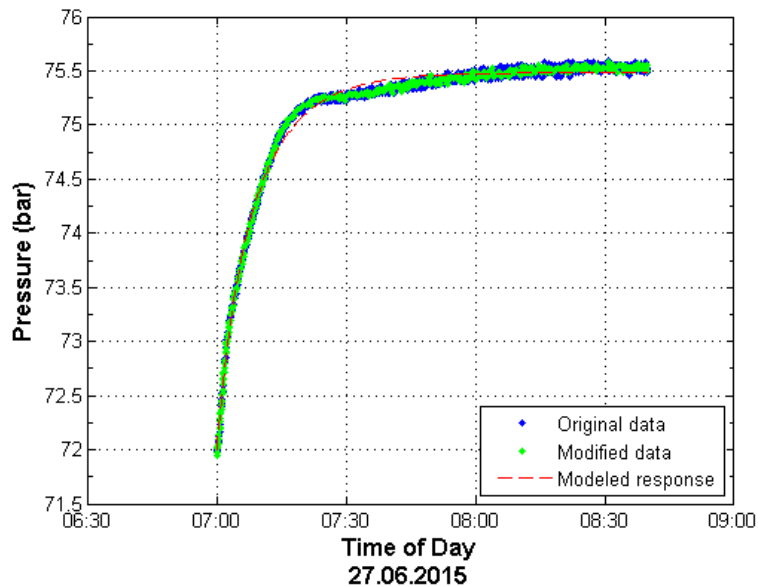


FIGURE 10: Well NJ-28. Simulated model (red line), selected data (green) and collected data (blue) for step 1

Figure 11 shows additional plots of the same data on a log-time scale and linear pressure scale (A), and a log-log scale with the modelled response of the data (B). This is used to determine which type of model is most applicable for each step.

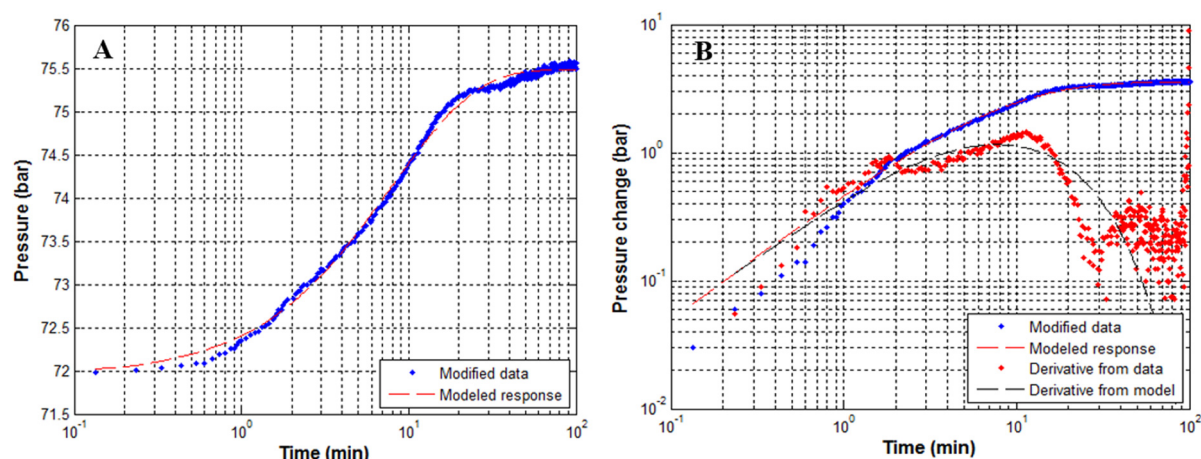


FIGURE 11: Well NJ-28. A) Simulated model, and collected data for step 1 using log-time scale; and B) On a log-log scale showing the derivatives of the same step (1) from a homogenous

4.2.2 Well injection test of NJ-13

The injection test at well NJ-13 consisted of 5 steps and was performed from the 21st – 22nd August 1985. The initial injection was constant with an injection rate of 26 l/s to stabilize the pressure in the well. The measurements of the pressure and temperature during the steps were performed at 1570 m depth which was believed to be close to the main feed zone of the well. Injection in step 1 started with 10 l/s, step 2 with 20 l/s, step 3 with 30 l/s, step 4 with 45 l/s and in step 5 with 0 l/s. Figure 12 shows the injection (Q) and the pressure (P) responses as well as their changes (ΔQ and ΔP) for each step.

In step 1, at around 01:10, the pressure dropped probably due to instable injection, but increased again before starting step 2. Steps 2, 3, and 4 show an increase in pressure at the respective injection rates and the injectivity index increased from 3.11 – to 5.11 (l/s)/bar. At 07:56 on the second day of the injection test, step 5, the final step in the test which was a fall off step was conducted.

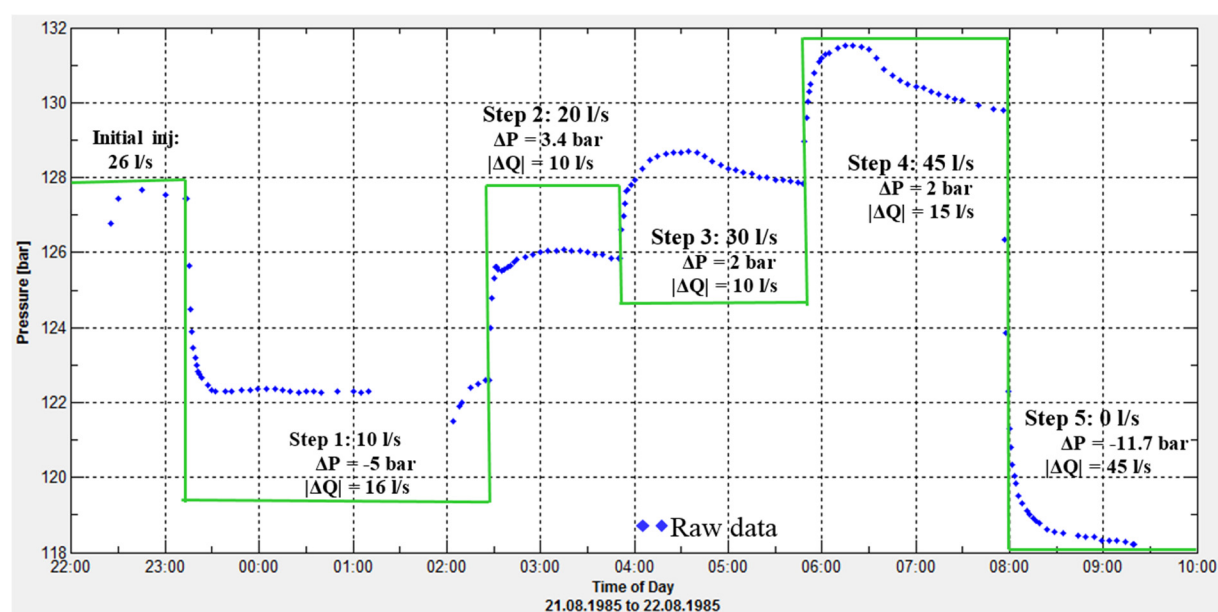


FIGURE 12: Pressure and injection as a function of time in well NJ-13 during the injection well test

The Well Tester software requires the input of some initial parameters and deduces the estimated reservoir pressure from the input data file. Table 6 shows all the initial parameter values of the reservoir that were used for this analysis.

Each of the steps was simulated using non-linear regression analysis separately and their respective parameters were estimated using Well Tester software (Table 7). Comparing the simulated results from Well Tester, steps 2, 3 and 4 in well NJ-13 turned out to give the best response for the selected model of *homogenous reservoir, constant pressure boundary, constant skin and wellbore storage*.

TABLE 6: Summary of initial parameters of well NJ-13

Parameter name	Value	Unit
Estimated reservoir temperature T	280	°C
Estimated reservoir pressure P	126	bar
Wellbore radius r_w	0.12	m
Porosity	0.1	-
Dynamic viscosity of reservoir fluid μ	9.55×10^{-5}	Pa·s
Compressibility of reservoir fluid c_w	1.97×10^{-9}	Pa ⁻¹
Compressibility of rock matrix c_r	2.44×10^{-11}	Pa ⁻¹
Total compressibility c_t	2.19×10^{-10}	Pa ⁻¹

TABLE 7: Summary of the results from the non-linear regression parameters estimated using injection test data from well NJ-13

	Step 1	Step 2	Step 3	Step 4	Step 5	Unit
Transmissivity T	3.0×10^{-8}	3.1×10^{-8}	4.0×10^{-8}	4.9×10^{-8}	7.3×10^{-8}	m ³ /(Pa·s)
Storativity S	3.6×10^{-9}	4.6×10^{-9}	2.2×10^{-9}	1.6×10^{-9}	2.1×10^{-9}	m ³ /(Pa·m ²)
Skin factor s	-0.8	-0.6	-1	-0.4	3.4	-
Wellbore storage C	3.7×10^{-6}	3.0×10^{-6}	6.6×10^{-6}	6.2×10^{-6}	5.7×10^{-6}	m ³ /Pa
Injectivity Index II	3.2	2.9	5	7.5	4	(l/s) / bar
Permeability thickness kh	2.7×10^{-12}	2.9×10^{-12}	3.9×10^{-12}	4.3×10^{-12}	7.2×10^{-12}	m·m ²

In the report by Steingrímsson et al., 1986, the model used to simulate the injection test for well NJ-13 calculated *dual porosity, infinite pressure boundary, constant well skin and wellbore storage*. However, the simulated values of the parameters attained in this injection analysis assuming a homogenous reservoir and constant pressure boundary (Table 7) do not defer much from the values given in the old report.

5. PRODUCTION WELL TESTING

5.1 Theoretical overview of production well testing

Production well tests for high-enthalpy geothermal wells are conducted after the well has been left to warm up for 2-4 months after completion to determine the energy content and production capacity and to analyse the flow characteristics of a well (Grant and Brixley, 2011). Furthermore, a production test may be necessary for developers of geothermal projects so that better utilization schemes can be proposed for each production well and to get information on how the reservoir should be managed in the future for better sustainability.

During the warm-up period, the well conditions become those of the surrounding rocks, so production test calculations after warm-up reflect the true energy status of the reservoir. However, it is also vital to bear in mind that other nearby wells may be affecting the results. Production well tests are done by

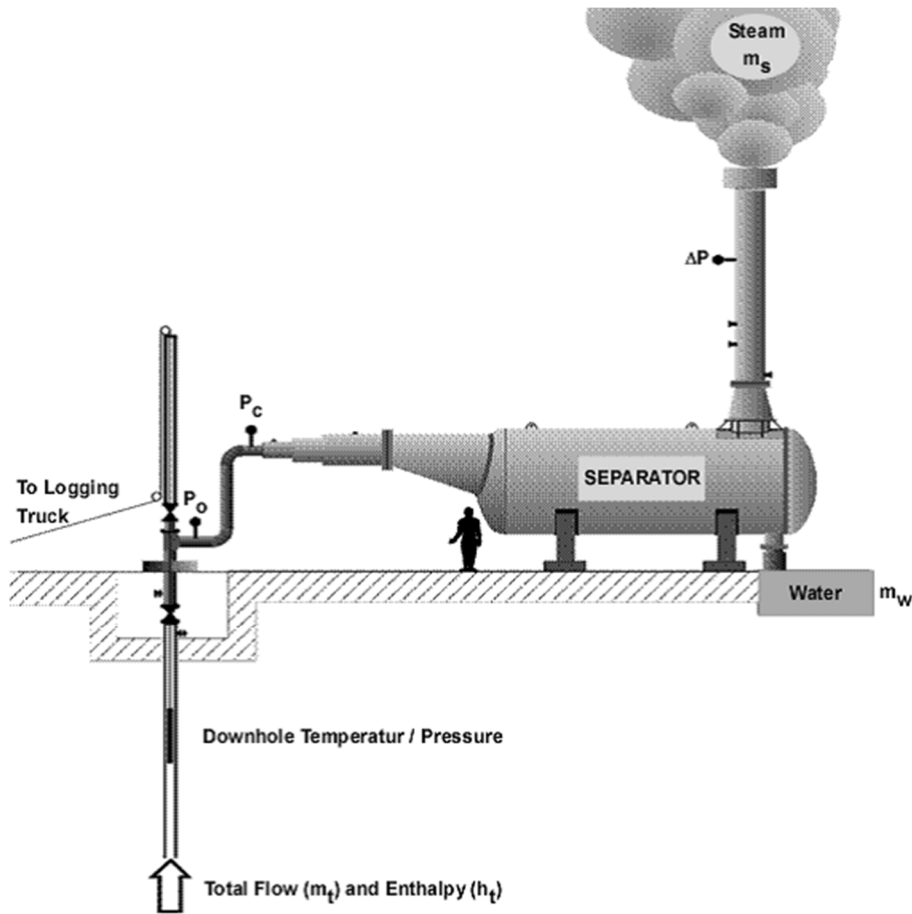


FIGURE 13: Production well test setup for flow and enthalpy measurements with a horizontal separator (Björnsson, et al., 1998)

measuring the fluid flow from a discharging well at different wellhead pressures. The fluid flow is discharged into a silencer or separator which is designed to reduce the noise level resulting from the discharge and it separates the fluid into steam and water at atmospheric pressures.

A typical setup for production well testing which is commonly used in Iceland is shown in Figure 13. The separator and equipment are connected to the well which is to be monitored. The lip pressure is measured at the end of the discharge pipeline as it enters the silencer and water discharged from the silencer or separator is collected in a V-notch weir box for measurements while the steam is discharged into the atmosphere. For well NJ-28 at Nesjavellir, a vertical steam separator was used but in Figure 13 a horizontal separator is shown.

The relation between mass flow, enthalpy, cross-sectional area of the discharge pipe and lip pressure is described by the Russell James's empirical formula below (Grant and Brixley, 2011):

$$Q_t = KA \frac{P_c^{0.96}}{H^{1.102}} \quad (14)$$

where Q_t = Total mass flow (kg/s);
 K = 183.5 when A is given in (cm²), i.e. K is not dimensionless;
 H = Total enthalpy (kJ/kg);
 A = Cross-section area of the pipe (cm²); and
 P_c = Lip pressure (bar-a).

Mass ratio of steam to the total flow and total enthalpy as a function of enthalpy of steam and water can be written as:

$$X = \frac{Q_s}{Q_t} \quad \text{and} \quad H = XH_s + (1 - X)H_w \quad (15)$$

where X = The steam mass fraction;
 Q_s = Mass flow of steam (kg/s);
 H_s = Enthalpy of steam (kJ/kg); and
 H_w = Enthalpy of water (kJ/kg).

The separated water flow Q_w describes the water separated at atmospheric pressure from the total well flow with enthalpy H . Therefore:

$$Q_t = Q_w \frac{H_s - H_w}{H_s - H} \quad (16)$$

where Q_w = Mass flow of water (kg/s).

Combining Equations 14 and 16 gives:

$$\frac{Q_w}{AP_c^{0.96}} = \frac{183.5}{H_t^{1.102}} \frac{H_s - H}{H_s - H_w} \quad (17)$$

The enthalpies of steam H_s and water H_w are found from steam-tables for corresponding well head pressure or temperature. The lip pressure P_c is measured during the production test. Figure 13 shows the set up. The total flow Q_t and the total enthalpy H can be calculated with algorithms solving non-linear equations.

The *LIP* programme from the ICEBOX software uses the Russell James equation (Equation 14) to find properties of two-phase geothermal wells. This programme was used to calculate the flow rates of both steam and water and their enthalpy.

5.2 Production well testing of NJ-13

A total of fourteen production test manual readings and measurements exist from 23rd September – 10th October 1985 during the production testing of well NJ-13. Table 8 shows the measurements from the production tests taken using a lip pipe diameter of 16.05 cm.

TABLE 8: Measurements of pressure at different times and water heights in well NJ-13

Date	Time	Water height W (cm)	Well head pressure P_o (bar-g)	Critical pressure P_c (bar-g)
23-Sep-85	20:20	23.4	17.0	3.40
23-Sep-85	20:25	23.6	16.0	3.80
23-Sep-85	21:15	23.6	15.5	3.70
23-Sep-85	23:20	23.3	15.0	3.60
24-Sep-85	13:00	21.3	16.5	4.10
24-Sep-85	17:00	20.8	16.7	3.80
26-Sep-85	15:00	9.2	20.5	4.40
27-Sep-85	11:45	11.3	16.2	4.18
29-Sep-85	15:00	10.3	15.8	4.40
30-Sep-85	22:00	10.2	16.2	4.50
05-Oct-85	11:20	8.9	16.3	4.50
07-Oct-85	11:35	7.7	16.4	4.70
10-Oct-85	14:00	8.0	16.3	4.50
10-Oct-85	18:35	8.2	16.7	4.40

The water height in the weir box W over the V-notch, well head pressure P_0 and the critical pressure P_c were manually entered into the Lip programme of the Icebox software to calculate the flow rates of steam Q_s and water Q_w . The total enthalpy H was calculated assuming the separator pressure to be 1 bar-g and 7 bar-g which are the separator pressure for the steam separator during testing and assumed separator pressure for the Nesjavellir power plant, respectively. The total flow rate Q_t is the sum of Q_s and Q_w .

Table 9 shows the results obtained using the Lip programme and the energy value calculated using a constant total steam flow rate of 2 kg/s for the production of 1 MWe. In general, the amount of steam needed for production of 1 MWe varies between 1.6 and 2.2 kg/s for different power plants. For a well head pressure P_0 of 16.4 bar-g the steam flow rate is 31 kg/s with a power output of 15 MW of electricity.

TABLE 9: Results of flow rate and enthalpy for well NJ-13

Date	Time	At 1 bar-a separator pressure				Enthalpy H (kJ/kg)	Q_s at 7 re	Power (MW _e)
		Q_w (kg/s)	Q_s (kg/s)	Q_t (kg/s)	X (%)			
23-Sep-85	20:20	37.4	20.5	57.9	35	1285	15.9	8.0
23-Sep-85	20:25	38.2	22.6	60.9	37	1324	17.9	9.0
23-Sep-85	21:15	38.2	22.1	60.3	37	1311	17.4	8.7
23-Sep-85	23:20	37.0	21.7	58.7	37	1318	17.1	8.6
24-Sep-85	13:00	29.7	25.6	55.3	46	1523	21.7	10.8
24-Sep-85	17:00	28.0	24.1	52.2	46	1524	20.4	10.2
26-Sep-85	15:00	4.1	30.6	34.6	88	2447	29.2	14.6
27-Sep-85	11:45	6.5	29.1	35.5	82	2305	27.5	13.8
29-Sep-85	15:00	5.3	30.4	35.7	85	2382	28.9	14.5
30-Sep-85	22:00	5.2	31.0	36.1	86	2393	29.5	14.8
05-Oct-85	11:20	3.8	31.1	34.9	89	2467	29.8	14.9
07-Oct-85	11:35	2.8	32.3	35.1	92	2531	31.1	15.5
10-Oct-85	14:00	3.0	31.2	34.2	91	2512	30.0	15.0
10-Oct-85	18:35	3.2	30.7	33.8	91	2500	29.4	14.7

5.3 Well NJ-28 production well testing

Measurements of temperature and pressure logged in the well during the production testing in September 2015 were not available when this report was finalised. A total of nine manual readings and measurements were carried out on the 14th September 2015 during the production test of well NJ-28.

Table 10 shows the manual measurements from the production test using a lip pipe diameter of 10 cm, the results obtained using the *LIP* programme and the energy value calculated using a constant total flow rate of 2 kg/s for the production of 1 MWe. From these results, it is estimated that NJ-28 could produce up to 5 MW_e for a wellhead pressure P_0 of 20 bar-g at a flow rate of 9.4 kg/s for 1 bar-a separator pressure. Table 10 shows that the mass fraction X of steam Q_s to the total flow Q_t calculated using Equation 15 is greater than 96 %. This indicates that the well produces mostly dry steam, hence it is not necessary to calculate the power output at 7 bar-a separator pressure.

The steam enthalpy H_s at 1 bar-a separator pressure and measured as 2675 kJ/kg, is slightly lower than at 7 bar-a separator pressure where it is 2762.7 kJ/kg. Calculations have shown that the power output (MW_e) is slightly less at 7 bar-a separator pressure than at 1 bar-a separator pressure. However, this does not change the results significantly and the well is estimated to produce mostly dry steam at well head pressures between 18-21 bar-g and could produce up to 5 MW_e at 7 bar-a, which is the assumed separator pressure for the Nesjavellir power plant.

TABLE 10: Manual production test measurements taken on 14th September 2015 and results of flow rate and enthalpy for well NJ-28 at flow rate of 2 kg/s for production of 1 MWe at 1 bar-a separator pressure

Time	Water height W (cm)	P_0 (bar-g)	P_c (bar-g)	Q_w (kg/s)	Q_s (kg/s)	Q_t (kg/s)	X (%)	Enthalpy H (kJ/kg)	Power MW _e
13:50	1.4	21.2	2.10	0.1	7.1	7.2	98	2665	3.5
13:55	3.0	20.1	3.20	0.4	9.4	9.8	96	2625	4.7
14:00	3.1	20.2	3.00	0.4	9.0	9.4	96	2618	4.5
14:05	3.0	19.5	2.20	0.3	7.6	7.9	96	2610	3.8
14:10	1.0	18.8	2.00	0.1	6.8	7.0	98	2671	3.4
14:15	0.8	18.4	2.00	0.1	6.8	7.0	98	2673	3.4
14:20	0.5	17.8	2.00	0.1	6.9	7.0	99	2675	3.4
14:25	1.4	18.0	2.60	0.2	8.2	8.3	98	2666	4.1
14:30	3.0	18.0	2.50	0.3	7.9	8.3	96	2615	4.0

6. CONCLUSIONS AND DISCUSSIONS

The main aim of this study was to analyse available temperature and pressure data and well tests from wells NJ-13 and NJ-28 in the Nesjavellir geothermal field in SW-Iceland. Well NJ-28 is a directional makeup well drilled from the same well pad as well NJ-13. Analysis of temperature and pressure profiles to find the formation temperature and initial pressure as well as analysis of injection and production well tests were the main methodologies applied to characterise various physical parameters of these two wells and the reservoir in their vicinity. The following conclusions have been made from the analysis of the two wells.

The formation temperature and initial pressure of NJ-13 at 1600 m depth, determined using BERGHITI, are 322°C and 116 bar-g, respectively. The formation temperature lies right on the boiling curve indicating a two-phase well. This is not far from conclusions of the previous analysis of well NJ-13 by Steingrímsson et al. (1986). For well NJ-28, the estimated initial pressure and the corresponding boiling point temperature are 65 bar-g and 281°C, respectively, at 1200 m vertical depth. The difference in the estimated initial pressure and formation temperature is 24 bar and 26°C, respectively, at the same depth (1200 m). The drawdown in the reservoir due to production cannot be estimated based on this difference because nearby wells, including well NJ-13, were in production when the warmup measurements were conducted.

Injection well test data from 5 steps in NJ-13 was simulated using Well Tester. The selected model was that of a *homogenous reservoir, constant pressure boundary, constant skin and wellbore storage* and showed that steps 2, 3 and 4 gave the best results.

The transmissivity in well NJ-13 generally increases with increasing injection rate in steps 2, 3 and 4. The injectivity index also increases from 2.9 to 7.5 (l/s)/bar in these 3 steps. This was explained by Steingrímsson et al. (1985) who believed this to be caused by more feed points becoming active when pressure was increased, especially from 900-1150 m depth.

All three steps for well NJ-28 were simulated using Well Tester and the best fit between modelled and measured data was obtained when using a *homogenous reservoir, constant pressure boundary, constant skin and wellbore storage*. The transmissivity and storativity were within the normal range of values in high-temperature reservoirs in Iceland. The injectivity index was slightly increasing in the step test from 4.0 to 4.3 (l/s)/bar, indicating a small opening up of the surroundings of the well during the test.

The older production well, NJ-13, drilled in 1985, has a power output of 15 MW_e estimated from the original production test data in September and October 1985. The recent well, NJ-28, which was directionally drilled from the same well pad in 2015, only has a power output of 5 MW_e estimated from production test data measured in September 2015. The mass fraction X of steam Q_s to the total flow Q_t calculated using Equation 15 is greater than 96% (Table 10). This indicates that the well produces mostly dry steam.

In general, the reservoir characteristics concluded from the interpretation of the injection tests of both wells NJ-13 and NJ-28 are fairly similar. However, well NJ-13 has both a higher transmissivity ranging from 4 to 5×10^{-8} m³/Pa.s, and an injectivity ranging from 5 to 7.5 (l/s)/bar compared to well NJ-28 which has a transmissivity ranging from 3 to 4×10^{-8} m³/Pa.s and an injectivity of ~4 l/s/bar. This might explain why the recent well, NJ-28, is a poor producer compared to the older well NJ-13.

ACKNOWLEDGEMENT

I would like to sincerely appreciate and thank my supervisors Dr. Svanbjörg Helga Haraldsdóttir, Saeunn Halldórsdóttir and Benedikt Steingrímsson for imparting their knowledge and experience in temperature and pressure, injection and production tests analysis and the applicable software used for each analysis. It is due to their tireless guidance and efforts that has led me through to the successful completion of this report.

Special thanks to the Orka nátturunnar (ON) and Iceland GeoSurvey (ISOR) for providing the well data of NJ-13 and NJ-28 which were used in this report.

I would also like to extend my special thanks to all the staff members of UNU-GTP under the stewardship of director Mr. Lúdvík S. Georgsson for the training opportunity, care and all the other associated privileges during the six months training programme. Extended appreciation to all the lecturers involved for imparting their knowledge and experiences through their presentations. Finally, I would like to appreciate and thank all the UNU-GTP Fellows for the moments we shared together.

NOMENCLATURE

A	= Cross section area of the pipe (cm ²)
C	= Wellbore storage (m ³ /Pa)
C_r	= Rock compressibility (Pa ⁻¹)
C_t	= Total compressibility (Pa ⁻¹)
C_w	= Water compressibility (Pa ⁻¹)
dr	= Thickness of shell/well (m)
h	= Reservoir thickness (m)
H_s	= Enthalpy of steam (kJ/kg)
H_t	= Total enthalpy (kJ/kg)
H_w	= Enthalpy of water (kJ/kg)
II	= Injectivity index ((l/s)/bar)
K	= 183.5 for A in cm ² at Reykjanes
k	= Permeability (m ²)
P	= Pressure (bar)
P_c	= Lip pressure (bar-a)
P_0	= Initial pressure or top-pressure (bar)
Q	= Mass flow (kg/s)
Q_s	= Mass flow of steam (kg/s)
Q_t	= Total flow rate (kg/s)

Q_w	= Mass flow of water (kg/s)
r	= Radius (m)
r_w	= Wellbore radius (m)
S	= Storativity ($\text{m}^3/\text{Pa}\cdot\text{m}^2$)
S	= Skin factor (-)
T	= Transmissivity ($\text{m}^3/(\text{Pa}\cdot\text{s})$)
W	= Water height in weigh box (cm)
X	= Steam mass fraction
ρ	= Density of fluid (kg/m^3)
φ	= Porosity
τ	= Horner time (-)
μ	= Fluid viscosity (Pa.s)
γ	= Euler constant

REFERENCES

- Arason, Th., Björnsson, G., Axelsson, G., Bjarnason, J.Ö., and Helgason, P., 2004: *The geothermal reservoir engineering software package Icebox, user's manual*. Orkustofnun, Reykjavík, report, 53 pp.
- Árnadóttir, T., Geirsson, H., and Jiang, W., 2008: Crustal deformation in Iceland: Plate spreading and earthquake deformation. *Jökull*, 58, 59-74.
- Árnason, B., Theodórsson, P., Björnsson, S., and Saemundsson, K., 1967: Hengill, a high-temperature thermal area in Iceland. *Bull. Volcanologique*, XXXIII-1, 245-260.
- Árnason, K., and Magnússon, I.Th, 2001: *Geothermal activity at Hengill and Hellisheidi. Results of electromagnetic soundings*. Orkustofnun, Reykjavík, Iceland, report OS-2001/091 (in Icelandic), 250 pp.
- Árnason, K., Eysteinnsson, H., Hersir, G.P., 2010: Joint 1D inversion of TEM and MT data and 3D inversion of MT data in the Hengill area, SW Iceland. *Geothermics*, 39, 13–34.
- Björnsson, G., 2004: Reservoir conditions at 3-6 km depth in the Hellisheidi geothermal field, SW-Iceland, estimated by deep drilling, cold water injection and seismic monitoring. *Proceedings of the 29th Workshop on Geothermal Reservoir Engineering, Stanford University, Stanford, CA, US*, 8 pp.
- Björnsson, G., Bjarnason, J.Ö., and Thórdarson S., 1998: *Discharge measurements in Svartsengi and Eldvörp in 1996-1997*. Orkustofnun, Reykjavík, Iceland, report OS-98008 (in Icelandic), 57 pp.
- Bödvarsson, G.S., Björnsson, S., Gunnarsson, Á., Gunnlaugsson, E., Sigurdsson, Ó., Stefánsson V., and Steingrímsson, B., 1990: The Nesjavellir geothermal field, Iceland. Part 1. Field characteristics and development of a three-dimensional numerical model. *J. Geotherm. Sci. and Tech.*, 2-3, 189-228.
- Bödvarsson, G.S., and Witherspoon, P.A., 1989: Geothermal reservoir engineering, part 1. *Geotherm. Scie & Tech*, 2-1, 1-68.
- Dowdle, W.L., and Cobb, W.M., 1975: Static formation temperature from well logs – an empirical method. *J. Petrol. Tech.*, 27, 1326-1330.
- Franzson, H. and Sigvaldason, H., 1985: *Nesjavellir well NG-8, geology, alteration, logging and aquifers*. Orkustofnun, Reykjavík, report OS-85120/JHD-16 (in Icelandic), 33 pp.

Franzson, H., and Steingrímsson, B., 2015: *The Hengill geothermal system – exploration, drilling, monitoring and modelling*. UNU-GTP, unpublished lecture notes, 102 pp.

Gíslason, G., 2000: Nesjavellir co-generation plant, Iceland. Flow of geothermal steam and non-condensable gases. *Proceedings of the World Geothermal Congress 2000, Kyushu-Tohoku, Japan*, 585-590.

Gíslason, G., and Gunnlaugsson, E., 2003: Preparation for a new power plant in the Hengill geothermal area. *IGA News*, 51, 4-5.

Grant, M.A., and Bixley, P.F., 2011: *Geothermal reservoir engineering* (2nd edition). Academic Press, NY, US, 359 pp.

Gunnarsdóttir, S., Helgadóttir, H.M., Tryggvason, H., Sigurgeirsson, M.Á., Egilson, Th., Stefánsson, H.O., 2015: *Nesjavellir – Well NJ-28; third stage: Drilling of production zone to 1301 m depth*. ÍSOR – Iceland GeoSurvey, Reykjavík, report ÍSOR-2015/033 (in Icelandic), 103 pp.

Gunnarsson, Á. Steingrímsson, B.S., Gunnlaugsson, E., Magnússon, J., and Maack, R., 1992: Nesjavellir geothermal co-generation power plant. *Geothermics*, 21, 559-583.

Helgason, P., 1993: *Step by step guide to BERGHITI. User's guide*. Orkustofnun, Reykjavík, Iceland, 17 pp.

Hjartarson, Á., 1999: *Analysis of reservoir data collected during reinjection into the Laugaland geothermal system in Eyjafjörður, N-Iceland*. MSc. thesis, University of Iceland and Orkustofnun, Reykjavík, 107 pp.

Horne, R.N., 1995: *Modern well test analysis, a computer aided approach* (2nd ed.). Petroway Inc., Palo Alto, CA, United States, 257 pp.

Jóhannesson H., and Saemundsson, K., 1999. Geological map 1:1.000.000, Icelandic Institute of Natural History.

Júlíusson, E., Grétarsson, G., Jónsson, P., 2007: *Well tester 1.0b, user's guide*. ÍSOR – Iceland GeoSurvey, Reykjavík, Iceland, report ÍSOR-2008/063, 27 pp.

Níelsson, S., and Franzson, H., 2010: Geology and hydrothermal alteration of the Hverahlíð HT-system, SW-Iceland. *Proceedings of the World Geothermal Congress 2010, Bali, Indonesia*, 6 pp.

Saemundsson, K., 1979: Outline of the geology of Iceland. *Jökull* 29, 7-28.

Steingrímsson, B., Gudmundsson, Á., Sverrisdóttir, G., Sigvaldason, H., Sigurdsson, Ó., Gunnlaugsson, E., 1986: *Nesjavellir, well NJ-13: Drilling, exploration and production characteristics*. Orkustofnun, Reykjavík, Iceland, report OS-86027/JHD-07, 145 pp.

Theis, C.V., 1935: The relation between the lowering of the piezometric surface and the rate and duration of discharge of a well using ground-water storage. *Transactions, American Geophysical Union*, 16-2, 519-524.

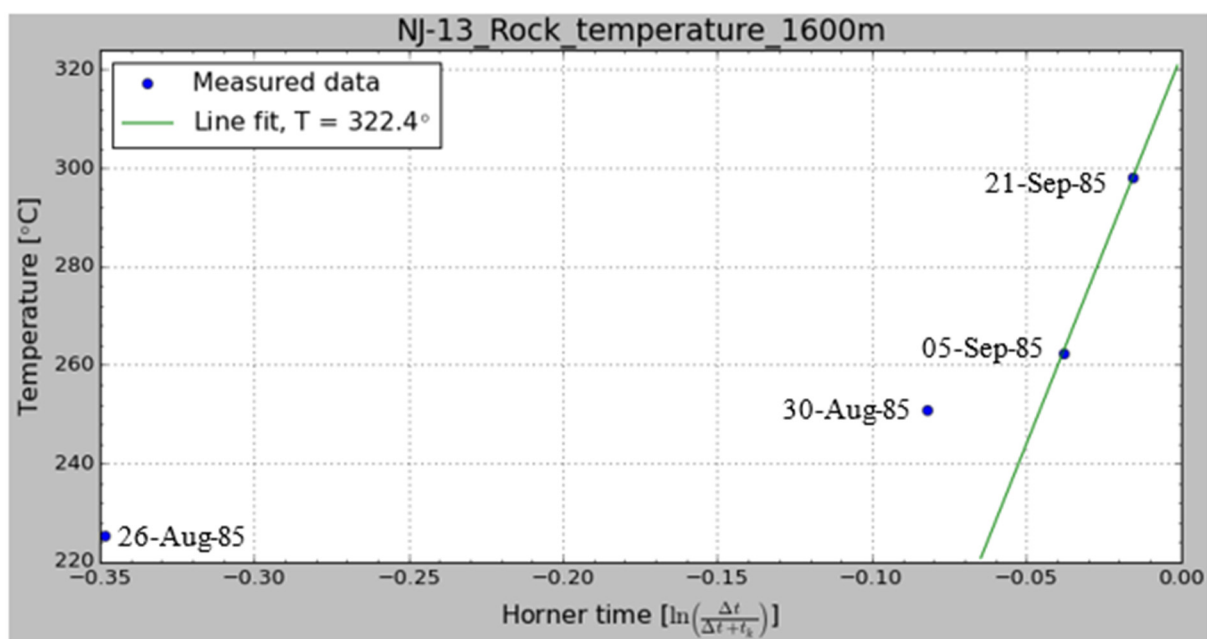
APPENDIX I: Estimation of formation temperature of well NJ-13

FIGURE 1: Estimation of formation temperature of well NJ-13 at 1600 m depth using BERGHITI